

Impact of multi-air plasma jets on nitrogen concentration variance in effluent of membrane bioreactor pilot-plant

Suthida Theeparaksapan¹⁾, Yanika Lerkmahalikhit¹⁾, Pichitchai Suwannapech²⁾, Prateep Boonnong²⁾, Mongkol Limawatchanakarn²⁾, and Khanit Matra^{*2)}

¹⁾Department of Civil and Environmental Engineering, Faculty of Engineering, Srinakharinwirot University, Nakhonnayok 26120, Thailand

²⁾Department of Electrical Engineering, Faculty of Engineering, Srinakharinwirot University, Nakhonnayok 26120, Thailand

Received 18 March 2021

Revised 25 April 2021

Accepted 14 May 2021

Abstract

An investigation of an atmospheric non-thermal air plasma effect on the modification of nitrogen concentration in the effluent of membrane bioreactor (MBR) pilot-plant has been proposed in this paper. The plasma treatment system has been a vertical liquid circulating system with horizontal multi-air plasma jets generated by a 125 W neon power supply. It has been found out that the variation trend of nitrogen concentration in air plasma-treated MBR effluent and deionized water (DI water) with different electrical conductivity (EC), ranging from 361.3 ± 21.3 to $2,153.3 \pm 83.1$ $\mu\text{S}/\text{cm}$, has been similar. The trend has been a positively skewed bell-like curve. The highest nitrogen concentration in the plasma-treated effluent has been found out at 15 min plasma treatment, which has been almost two times higher than that of the untreated effluent. The experimental results show that the EC of treated media had not significantly influenced the nitrogen concentration variance. However, considerably low EC (less than 1 $\mu\text{S}/\text{cm}$) of liquid media affects the difficulty of plasma generation. Regarding the experimental results, the atmospheric non-thermal air plasma has shown a positive impact on the nitrogen enhancement of MBR effluent, which could provide information in water reuse applications.

Keywords: Air discharge, Wastewater treatment, Membrane bioreactor (MBR), Circulating system, Water reuse

1. Introduction

The membrane bioreactor (MBR) system is a novel effective wastewater treatment technology that offers many advantages, including excellent effluent quality, stable operation performance, a small footprint, and reduction of excess sludge production [1, 2]. Although MBR technology is well-positioned to play a critical role in reuse applications, the MBR effluent has not met the water reuse standard for human consumption [3]. Among the existing utilization of reclaimed water, the reuse of MBR effluent for the agricultural farm would also be another practical application [1]. However, regarding the effective treatment system of MBR, the essential plant nutrient concentration in the effluents, such as nitrogen (N) and phosphorus (P), is usually low, and this does not meet the requirement for plant growth. Even though applying fertilizer directly into the water is the most efficient method, it could result in the long term side-effect of an environmental issue caused by chemical fertilizers [4, 5].

Recently, an atmospheric non-thermal plasma (ANTP) has been promoted as a novel technology for advanced oxidation processes (AOPs) applications in water and liquid treatment [6-9]. Regarding the AOPs, many reactions and byproduct chemical substances could be achieved depending on the plasma experimental conditions, the plasma model configuration, the treatment time, the generation power, and the carrier gas, including the target liquid chemical compounds. Some notable ANTP applications in water treatment are chemical decontamination, microorganism disinfection, water quality improvement, plasma-activated water for the bio-medical treatment or sterilization, and liquid fertilizer for agricultural applications [6-8, 10-14]. Besides various beneficial reactive oxygen species (ROS) and reactive nitrogen species (RNS), other phenomena that have occurred during the plasma treatment process, such as ultraviolet (UV) radiation, photon ($h\nu$), electric field (EF), and shock wave, could also contribute in water quality enhancement [9, 12, 15, 16].

In this paper, the influence of the ANTP by multi-air plasma jets on nitrogen concentration modification in MBR effluent has been investigated. The possibility of an enhancement of nitrate-nitrogen ($\text{NO}_3\text{-N}$) concentration in MBR effluent by air plasma treatment for liquid fertilizer or liquid disinfectant (in the form of unstable structural nitrate isomer) in agriculture has been studied. The plasma treatment system has been designed as a liquid circulating system. The pumped liquid stream released at the top of the treatment system would be directly treated by multi-air plasma jets falling into the reservoir container. This would increase the plasma contact surface ratio and the probability to be directly treated with the target liquid. The treated liquid temperature could be significantly decreased, compared to the static treatment system [9, 10], owing to the thermal diffusion to the ambient air during the circulation. Moreover, the problem of dielectric relaxing time and liquid conductivity tolerance, for long time operation, affecting plasma generation in the in-liquid discharge system could be neglected since the air gap distance between electrodes would be kept constant [17, 18]. The variation

*Corresponding author. Tel.: +66 2649 5000 ext. 27088

Email address: khanit@gs.wu.ac.th

doi: 10.14456/easr.2021.75

of plasma treatment time on the target MBR effluent treatment on nitrogen concentration has been investigated comparing it with the control-deionized water. The effect of electrical conductivity (EC) of the deionized water (DI water) on nitrogen concentration variation due to plasma treatment has been investigated. The air plasma jets and other physicochemical parameters of liquid such as pH, EC, oxidation-reduction potential (ORP), temperature, and dissolved oxygen (DO) have been also investigated.

2. Materials and methods

2.1 Plasma model and experimental setup

The proposed plasma-activated water treatment system has been designed in a circulating treatment system as illustrated in Figure 1(a). The target liquid stored in the reservoir container has been pumped by a 600 ml/min water pump to the 0.5Ø cm three-way joint quartz tube located at the top of the treatment system. At this water flow rate, the water stream has been visually observed as a stable laminar flow. A copper wire has been inserted into the center of the three-way joint as an electrode. When the water pump has been operated, the copper wire has been immersed in a target liquid. The liquid stream has fallen vertically to the reservoir container and pumped back to the top of the treatment system. Three syringe needles as plasma jet nozzles have been hooked on the exoskeleton of the plasma treatment system surrounding the target water stream. The needle tip has been far from the water stream for 1.5 cm, approximately. Three needles have been arranged radially symmetric surrounding the water stream. However, they have not been arranged at the same level. The distance between each needle has been 2 cm, horizontally. Fifteen lpm of air from the air pump have been supplied to every needle via a plastic tube. The center of the syringe needle tip has been rotated 10 degrees clockwise from its basement (the axial direction from the needle tip axis has been in a tangent line of the water stream surface) in order to avoid water stream interruption from the flowing air. A terminal of 15 kV from a commercial neon transformer (125W commercial neon transformer, Topneon, TPN-1520A) has been connected to the copper wire electrode. In contrast, another terminal has been grounded and connected to the 100-ohm monitor resistor in series before connecting it with three parallel syringe needle electrodes. The target liquid has been treated at different treatment times at 0 (control group), 15, 30, 45, and 60 mins in the open environment.

The electrical characteristics of discharge waveforms have been recorded by an oscilloscope (SIGLENT, SDS2304). A high voltage probe (Pintek HVP-39 pro) has been connected across the anode and the ground electrode in order to monitor discharge voltage (V_d) characteristics. The discharge current (I_d) waveform has been retrieved from the voltage dropped across the monitor resistor. A charge-coupled device (CCD) spectrometer (Newport 71SI00087) has been used to observe the optical emission spectroscopy (OES). An optical detector has been perpendicularly located at the center between the needle tip and the water stream. The detector tip has been far from the plasma jet for 1 cm, approximately.

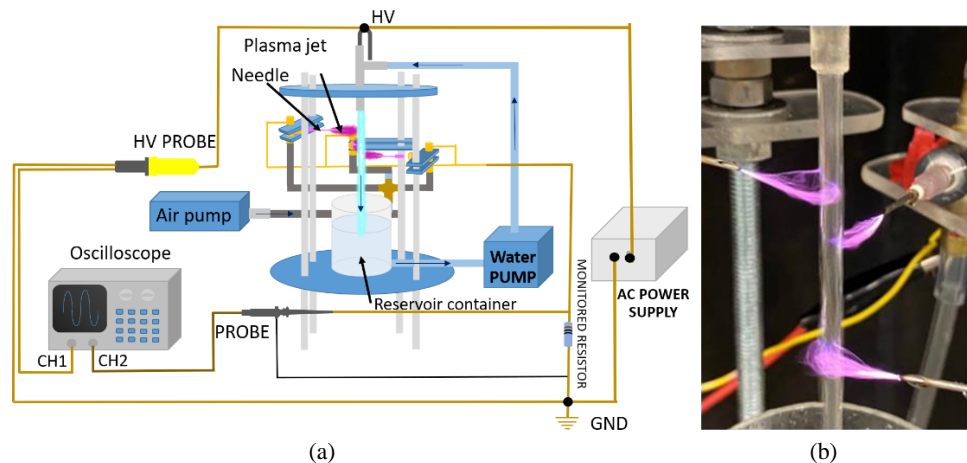


Figure 1 (a) A schematic drawing of the plasma model and the experimental setup, and (b) Image of MBR water stream being treated by multi-air plasma jets.

2.2 The effluent of the MBR pilot-plant

These investigations have been conducted using all the samples from the MBR pilot-plant, which has received mainly wastewater from a household building in Nakhon Nayok, Thailand. It has been installed to treat up to 9.6 m³ of wastewater per day. The membrane has been a submerged microfiltration hollow fiber membrane with a nominal pore size of 0.1 µm from Sumitomo Electric Company, Japan. The total membrane area of each membrane has been 6 m², and six membrane units have been installed. The water quality parameters of the MBR effluent from the plant used in this study are shown in Table 1.

Table 1 Water quality of MBR effluent

Parameters	Unit	Value
pH	-	7.0 ± 0.4
EC	µS/cm	649.3 ± 92.7
COD	mg/l	19.2 ± 12.0
Total Nitrogen (TN)	mg/l	21.5 ± 3.6
Nitrate-Nitrogen (NO ₃ - N)	mg/l	17.9 ± 2.4
Total phosphorus (TP)	mg/l	1.2 ± 0.5

2.3 Laboratory analyses

The physicochemical parameters have been characterized before and after the treatment. The pH levels, the temperature, and the DO have been measured using a Portable pH-DO meter (model HandyLab 100, SI Analytics). The EC and the ORP have been measured using a conductivity meter (model HI4321, Hanna). Samples have been collected periodically from the flasks in order to determine nitrate-nitrogen ($\text{NO}_3\text{-N}$), ammonium-nitrogen ($\text{NH}_3\text{-N}$), and total nitrogen (TN) concentrations. TN and $\text{NH}_3\text{-N}$ analyses have been performed using Hach-Lange cuvettes and a DR900 spectrophotometer (Hach-Lange, Belgium), while the Environment Protection Authority (EPA) has performed $\text{NO}_3\text{-N}$ analyses Approved Brucine Method.

2.4 Statistical analyses

The experimental data have been obtained from triplicated experiments ($n = 3$). The experiment has compared the characteristic values using one-way analysis of variance (One way-ANOVA). A p -value lower than 0.05 ($p < 0.05$) within groups has been considered.

3. Results

3.1 Air plasma jet characteristics

After the airflow rate and the gap distance have been adjusted optimally to the supplied source voltage from a neon transformer as mentioned in the experimental setup, air plasma jets have been uniformly generated between the needle tips and the water stream [13, 19]. The air plasma jet characteristic is illustrated in Figure 1(b). It has been a streamer-like discharge with a transient spark discharge as the intensified purple filaments could be noticed in the plasma stream. The air jets have been blown along with the axial needle axis. However, the air plasma plumes have been attracted to the water stream surface due to the electrical driven between the needle tips and the water stream [20, 21]. Therefore, it could be implied that the air plasma jets could effectively interact with the continuously flowing water stream surface.

Regarding the circulating plasma treatment, the treated water temperature could be greatly decreased compared to the static treatment. After 60 min of treatment, the plasma-treated water temperature has been around 42.5° Celsius, which is approximately 6.5° Celsius lower than the one of the 15 min static treatment. Moreover, target water could have interacted with air plasma jets thoroughly.

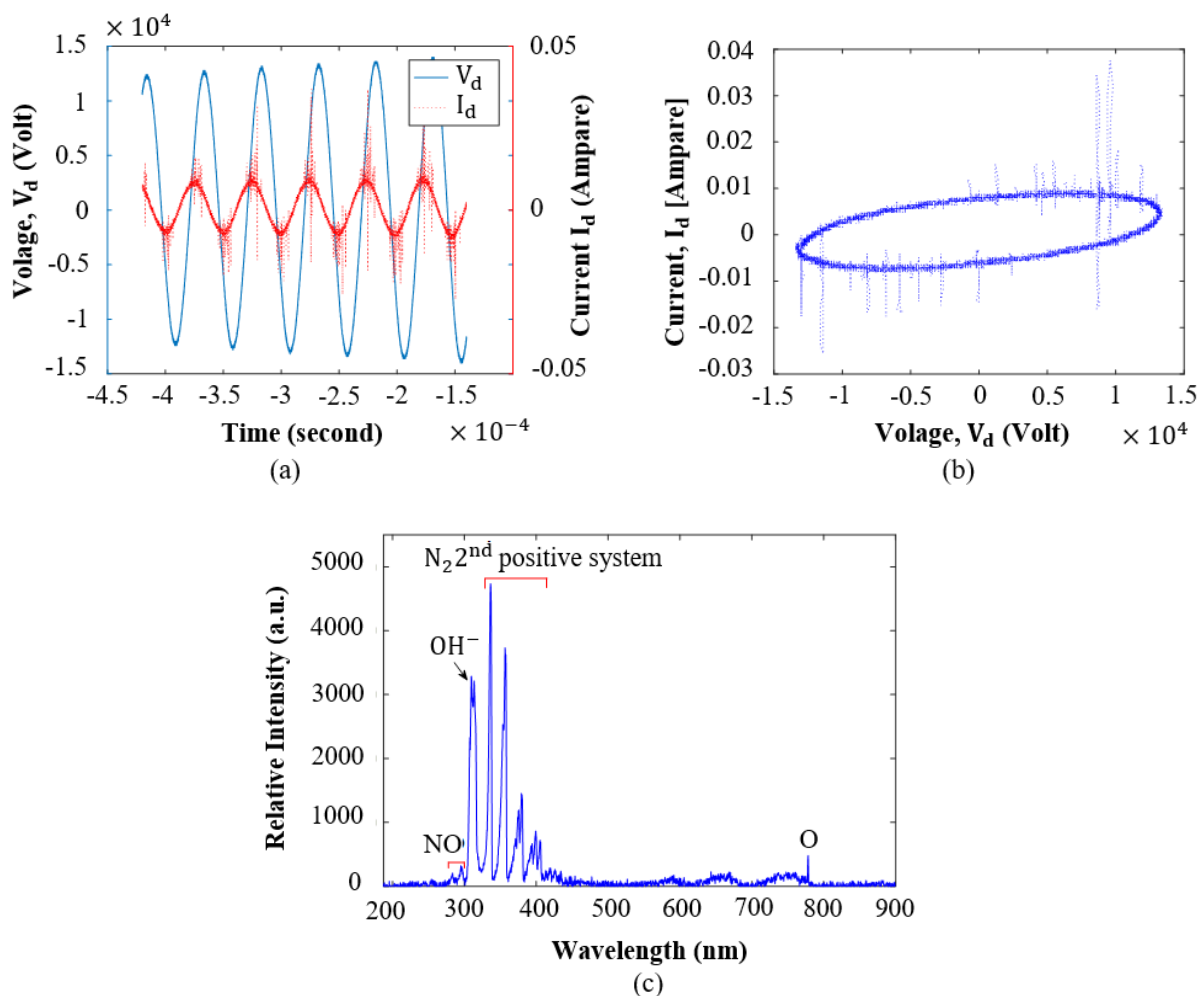


Figure 2 (a) Electrical characteristics of voltage and current waveforms, (b) The voltage and current plot over one period, and (c) Optical emission spectra of air plasma jets.

The electrical waveforms of voltage across the plasma jets and a current flowing in the treatment system are presented in Figure 2(a). The voltage and the current have been out of phase owing to the capacitive plasma load. The voltage across the plasma model has been $9.26 \text{ kV}_{\text{rms}}$, with the peak voltage around 13.45 kV . The voltage frequency has been 20 kHz , while the micro discharge current frequency has been 10 MHz , approximately. The primary conducting current flowing through the plasma has been about $7 \text{ mA}_{\text{rms}}$ with the micro discharge pulses ranging from $12\text{--}37 \text{ mA}_{\text{rms}}$ generated during the rising edge of every half-cycle. Figure 2(b) presents the voltage-current (V-I) plot over one period of air plasma jets. It could be noticed that the average micro discharges in the negative cycle have been comparatively lower than the positive cycle owing to the space charge effect between the electrodes. Therefore, it could be implied that the discharge power dissipation is an asymmetry in each half voltage period [22, 23]. The optical emission spectrum (OES) could be observed regarding these micro discharges, as illustrated in Figure 2(b).

Various optical emission spectrums could be detected by OES investigation during air plasma generation, as shown in figure 2(c). The second positive system of N_2 could be observed in the range of $300\text{--}400 \text{ nm}$. The atomic oxygen emission line has been detected at 777.4 nm . Moreover, the hydroxyl ion (OH^\cdot) radical emission lines at 309.6 nm , and the $\text{NO } \gamma$ bands ranging from $270\text{--}295 \text{ nm}$ have been noticed [24-27]. These radicals play an essential factor as a primary reactive species resulting in other by-product reactive oxygen and nitrogen species (RONs) which are beneficial for the water treatment process, such as hydroxyl radical (OH^\cdot), superoxide anion (O_2^\cdot), hydrogen peroxide (H_2O_2), ozone (O_3), nitric oxide (NO), Peroxynitrous acid (ONOOH), and peroxyxynitrite (ONOO^\cdot).

3.2 Nitrogen concentration variance during plasma treatment

In order to investigate the impact of air plasma on nitrate-nitrogen conversion, it is necessary to compare it with the control water media. In this time, a commercial deionized DI water (Maxzaa®, LCH Chemical, Thailand) has been used as the control group. However, at the same experimental condition of plasma generation, air plasma could not be generated between the needle and the DI water stream [17, 18, 28-32]. This is because the DI water has a very low EC (less than one $\mu\text{S}/\text{cm}$). It should be noted here that the proposed treatment system is a gas-liquid-phase discharge, in which liquid media serves as a cathode in every half-cycle [33]. Since the cathode is the major secondary electron emission source to sustain the discharge [32, 33], the electrode's conductivity has played an essential role in the gas discharge process. In order to generate gas discharge between the very low EC (quasi-nonconductive) electrodes, very high supplied voltage is required, compared to the conductive electrode [17, 18, 28-32]. Therefore, the EC of the DI water has been adjusted by adding potassium chloride (KCl), which is a common standard electrolyte used for EC adjustment of electrochemistry solutions, until the EC level has been closed to the one of the target MBR water ($649.3 \pm 93 \mu\text{S}/\text{cm}$) [18, 29, 30]. However, in order to confirm whether KCL has influenced the nitrate-nitrogen conversion, the DI waters with various dissolved KCl concentrations have been treated by multi-air plasma jets and investigated.

The concentrations of total nitrogen (TN), ammonia-nitrogen ($\text{NH}_3\text{-N}$), and nitrate-nitrogen ($\text{NO}_3\text{-N}$) have been measured immediately after the treatment process of each experiment. The result has shown that $\text{NH}_3\text{-N}$ has not been detected in any sample tested, because any residual ammonia-nitrogen has been likely oxidized to another form of nitrogen. The $\text{NO}_3\text{-N}$ and the TN concentrations are plotted against plasma treatment time, as shown in Figure 3. For both samples, nitrate-nitrogen has been induced upward at a contact time of 15 min and then declined (positively-skewed bell curve). However, it can be observed that the initial concentration of $\text{NO}_3\text{-N}$ and TN in MBR is higher than the one of the EC-adjusted DI water. This will be discussed again in section 4.3. The maximum concentrations of nitrate-nitrogen and total nitrogen of MBR effluent after 15 min plasma treatment have been $31.10 \pm 2.44 \text{ mg/l}$ and $33.80 \pm 0.60 \text{ mg/l}$, respectively, which are higher than the initial concentrations around 1.74 and 1.68 times, respectively. Moreover, these ones are higher than the ones of $649.3 \pm 93 \mu\text{S}/\text{cm}$ DI water around 1.13 , and 1.21 times, respectively.

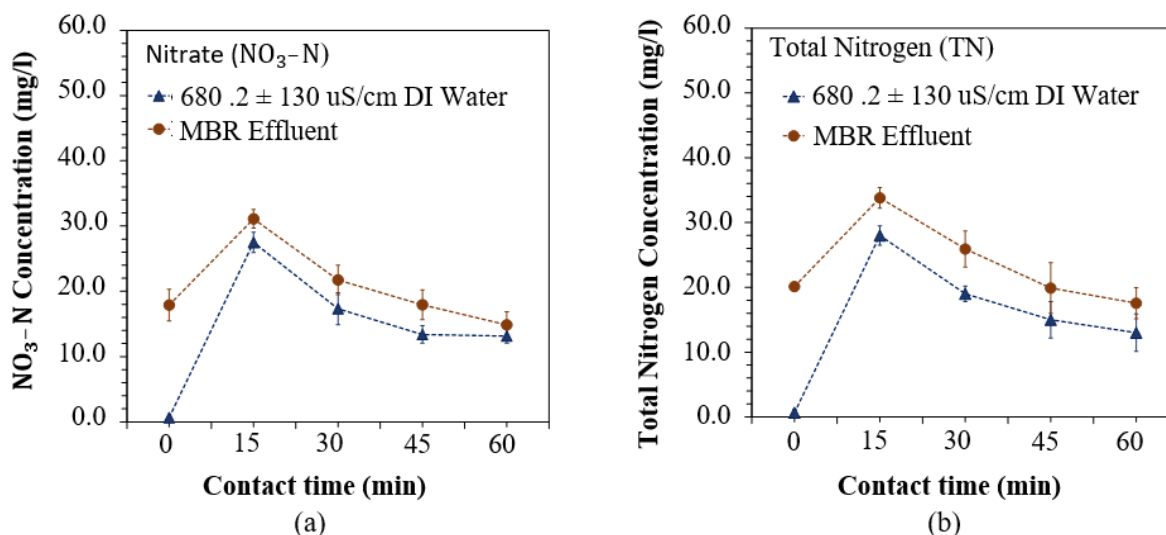


Figure 3 (a) Nitrate-nitrogen concentration, and (b) Total nitrogen concentration in MBR effluent and EC-adjusted DI water at various treatment times.

The effect of the parameters on the performance of plasma in liquid samples has been studied. Figure 4 presents the variance of the operating parameters, which are pH, EC, ORP, and DO, after plasma treatment at various treatment times. It could be seen that all the parameters of both conditions have the same trend. The DO concentration and the pH have been declined, while EC and ORP have been increased when the treatment time increased. It could be noticed that the pH and the ORP of both cases have seemed to saturate around 3.15 , and 548.95 mV , respectively. This has happened possibly because the chemical compounds have reached a stable state [34].

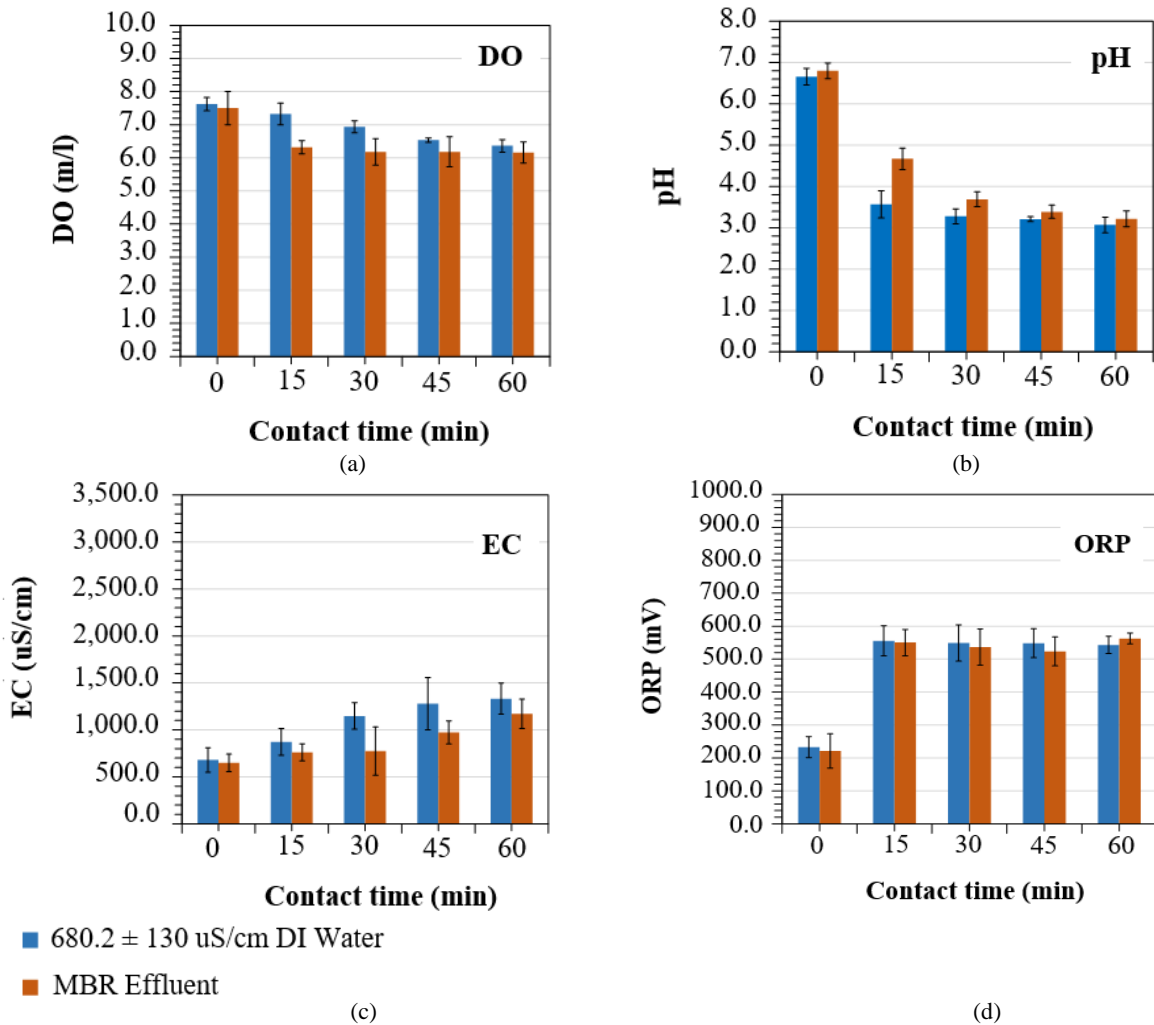


Figure 4 (a) DO, (b) pH, (c) EC, and (d) ORP of liquid media samples after air plasma treatment at various treatment times.

3.3 Effect of potassium chloride during plasma treatment

In order to study the effect of KCl concentration on the nitrate-nitrogen conversion during plasma treatment, the KCl solution has been prepared with different levels of concentration at 2, 4, 6, and 12 mol/l, resulting in the EC of DI water become 361.3 ± 21.3 , 700.2 ± 23.5 , 1265.7 ± 83.1 , 2153.3 ± 83.1 $\mu\text{S/cm}$ respectively. The nitrate nitrogen concentration of every KCl concentration has been rapidly increased during the first 15 min and then gradually declined, as illustrated in Figure 5. It can be observed that the trend has been also the positively skewed bell curve. From the experimental results and the statistical analysis in this study, it could be implied that the KCl (in the range mentioned above) dissolved in DI water has not significantly affected nitrate-nitrogen yield. However, it could enhance the plasma generation in terms of increasing the electrical conductivity of the liquid electrode, as discussed in section 3.2 [17, 18, 28-32].

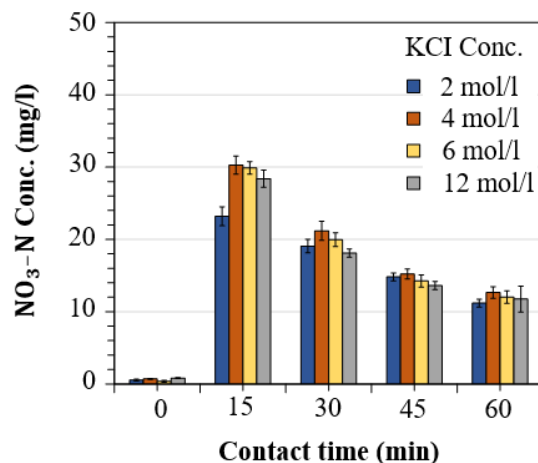


Figure 5 The changes of nitrate-nitrogen yield in various KCl concentrations during air plasma treatment at various treatment times.

of ONOOH, which is much more reactive than ONOO⁻. These results also show a possible role of acidified nitrite on plasma-induced microbial inactivation. However, the detailed mechanism of plasma-induced acidified nitrite needs further investigation.

5. Conclusions

This study has demonstrated that an atmospheric non-thermal air plasma jet could be applied possibly and effectively in order to improve the nitrogen concentration in MBR effluent. The effect of treatment time on treatment efficiency has been investigated. The results indicate that an optimum plasma treatment time in this study has been 15 min resulting in the highest percent of the enhancement. The reduction of nitrate-nitrogen after a long-time plasma treatment can also provide essential knowledge for the possibility of nitrate removal by air plasma. It has been found out that the variations of EC of treated liquid media have not significantly affected nitrate-nitrogen yield, but it has enhanced the plasma generation. It has been hypothesized that the enhancement of nitrate is due to the formation of atomic species (N and O) in the air discharge, which can be further oxidized to NO₂ and NO₃. From this study, it could be confirmed that not only air plasma could enhance nitrate-nitrogen concentration in the MBR effluent, which could be employed as liquid fertilizer, but an acidified nitrite in the air plasma treated MBR effluent could also be possible for microbial inactivation.

6. Acknowledgements

This work was supported by the faculty of engineering, Srinakharinwirot University.

7. References

- [1] Tang CY, Yang Z, Guo H, Wen JJ, Nghiem LD, Cornelissen E. Potable water reuse through advanced membrane technology. *Environ Sci Tech*. 2018;52(18):10215-23.
- [2] Judd S. *The MBR book: principles and applications of membrane bioreactors for water and wastewater treatment*. 2nd ed. Netherlands: Elsevier; 2010.
- [3] Crook J, Ammerman D, Okun D, Matthews R. *Guidelines for water reuse*. Washington: Environmental Protection Agency; 2012.
- [4] Chandini, Kumar R, Kumar R, Prakash O. The impact of chemical fertilizers on our environment and ecosystem. *Research trends in environmental sciences*. 2nd ed. India: AkiNik Publications; 2019. p. 69-86.
- [5] Bijoor N, Czimczik C, Pataki D, Billings S. Effects of temperature and fertilization on nitrogen cycling and community composition of an urban lawn. *Glob Chang Biol*. 2008;14(9):2119-31.
- [6] Matra K, Tawkaew S. Decolorization of methylene blue in an Ar non-thermal plasma reactor. *J Eng Sci Tech Rev*. 2020;13(1):114-9.
- [7] Deng Y, Zhao R. Advanced oxidation processes (AOPs) in wastewater treatment. *Curr Pollut Rep*. 2015;1(3):167-76.
- [8] Zhang Q, Zhang H, Zhang Q, Huang Q. Degradation of norfloxacin in aqueous solution by atmospheric-pressure non-thermal plasma: Mechanism and degradation pathways. *Chemosphere*. 2018;210:433-9.
- [9] Theeparaksapan S, Matra K. Atmospheric argon plasma jet for post-treatment of bio treated landfill leachate. 2018 International Electrical Engineering Congress (iEECON); 2018 Mar 7-9; Krabi, Thailand. New York: IEEE; 2018. p. 1-4.
- [10] Dechthummarong C, Matra K. An investigation of plasma activated water generated by 50 Hz half wave ac high voltage. 2018 International Electrical Engineering Congress (iEECON); 2018 Mar 7-9; Krabi, Thailand. New York: IEEE; 2018. p. 1-4.
- [11] Kaushik N, Ghimire B, Li Y, Adhikari M, Veerana M, Kaushik N, et al. Biological and medical applications of plasma-activated media, water and solutions. *Biol Chem*. 2018;400(1):39-62.
- [12] Simeckova J, Krema F, Klofac D, Dostal L, Kozakova Z. Influence of plasma-activated water on physical and physical-chemical soil properties. *Water*. 2020;12(9):2357.
- [13] Kucerova K, Henselova M, Slovakova L, Hensel K. Effects of plasma activated water on wheat: germination, growth parameters, photosynthetic pigments, soluble protein content, and antioxidant enzymes activity. *Plasma Process Polym*. 2019;16(3):1800131.
- [14] Tanakaran Y, Luang-In V, Matra K. Effect of atmospheric pressure multicorona air plasma and plasma-activated water on germination and growth of rat-tailed radish seeds. *IEEE Trans Plasma Sci*. 2021;49(2):563-72.
- [15] Sun B, Xin Y, Zhu X, Gao Z, Yan Z, Ohshima T. Effects of shock waves, ultraviolet light, and electric fields from pulsed discharges in water on inactivation of *Escherichia coli*. *Bioelectrochemistry*. 2018;120:112-9.
- [16] Lukes P, Clupek M, Babicky V, Sunka P. Ultraviolet radiation from the pulsed corona discharge in water. *Plasma Source Sci Tech*. 2008;17(2):24012-11.
- [17] Sunka P. Pulse electrical discharges in water and their applications. *Phys Plasma*. 2001;8:2587-94.
- [18] Wang H, Wandell R, Tachibana K, Vorac J, Locke BR. The influence of liquid conductivity on electrical breakdown and hydrogen peroxide production in a nanosecond pulsed plasma discharge generated in a water-film plasma reactor. *J Phys Appl Phys*. 2019;52(7):075201.
- [19] Ghosh S, Bishop B, Morrison I, Akolkar R, Scherson D, Mohan Sankaran R. Generation of a direct-current, atmospheric-pressure microplasma at the surface of a liquid water microjet for continuous plasma-liquid processing. *J Vac Sci Tech*. 2015;33(2):021312.
- [20] Xian Y, Lu X, Wu S, Chu P, Pan Y. Are all atmospheric pressure cold plasma jets electrically driven?. *Appl Phys Lett*. 2012;100(12):4-7.
- [21] Mohamed AAH, Aljuhani MM, Almarashi JQM, Alhazime AA. The effect of a second grounded electrode on the atmospheric pressure argon plasma jet. *Plasma Res Express*. 2020;2(1):1-21.
- [22] Nikiforov A, Sarani A, Leys C. The influence of water vapor content on electrical and spectral properties of an atmospheric pressure plasma jet. *Plasma Source Sci Tech*. 2011;20(1):015014.
- [23] Riba JR, Morosini A, Capelli F. Comparative study of ac and positive and negative dc visual corona for sphere-plane gaps in atmospheric air. *Energ*. 2018;11(10):2671.
- [24] Chen Z, Lin L, Cheng X, Gjika E, Keidar M. Effects of cold atmospheric plasma generated in deionized water in cell cancer therapy. *Plasma Process Polym*. 2016;13(2):1151-6.
- [25] Vlad IE, Anghel SD. Time stability of water activated by different on-liquid atmospheric pressure plasmas. *J Electrostat* 2017;87:284-92.

- [26] Cheng X, Sherman J, Murphy W, Ratovitski E, Canady J, Keidar M. The effect of tuning cold plasma composition on glioblastoma cell viability. *PLoS One*. 2014;9(5):e98652.
- [27] Walsh JL, Kong MG. Contrasting characteristics of linear-field and cross-field atmospheric plasma jets. *Appl Phys Lett*. 2008;93:111501.
- [28] Saito G, Nakasugi Y, Akiyama T. Generation of solution plasma over a large electrode surface area. *J Appl Phys*. 2015;118(2):023303.
- [29] Alteri GB, Bonomo M, Decker F, Dini D. Contact glow discharge electrolysis: effect of electrolyte conductivity on discharge voltage. *Catalysts*. 2020;10(10):1104.
- [30] Chokradjaroen C, Jiangqi N, Panomsuwan G, Saito N. Insight on solution plasma in aqueous solution and their application in modification of chitin and chitosan. *Int J Mol Sci*. 2021;22(9):4308.
- [31] Qazi HI, Xin Y, Li H, Khan M, Zhou L, Bao C. Effects of liquid electrical conductivity on the electrical and optical characteristics of an Ac-excited argon gas-liquid-phase discharge. *IEEE Trans Plasma Sci*. 2018;46(8):2856-64.
- [32] Bogaerts A, Neyts E, Gijbels R, Van der Mullen J. Gas discharge plasmas and their applications. *Spectrochim Acta B Atom Spectros*. 2002;57(4):609-58.
- [33] Muehe CE. AC breakdown in gases. Technical report. Massachusetts: Massachusetts Institute of Technology; 1965.
- [34] Thirumdas R, Kothakota A, Annapure U, Siliveru K, Blundell R, Gatt R, et al. Plasma activated water (PAW): chemistry, physico-chemical properties, applications in food and agriculture. *Trends Food Sci Tech*. 2018;77:21-31.
- [35] Lu X, Naidis GV, Laroussi M, Reuter S, Graves DB, Ostrikov K. Reactive species in non-equilibrium atmospheric-pressure plasmas: generation, transport, and biological effects. *Phys Rep*. 2016;630:1-84.
- [36] Suslow TV. Oxidation-reduction potential (ORP) for water disinfection monitoring, control, and documentation. ANR Publication. 2004;8149:1-5.
- [37] Wu Y, Bu L, Duan X, Zhu S, Kong M, Zhu N, et al. Mini review on the roles of nitrate/nitrite in advanced oxidation processes: radicals transformation and products formation. *J Clean Prod*. 2020;273(18):123065.
- [38] Judee F, Simon S, Bailly C, Dufour T. Plasma-activation of tap water using DBD for agronomy applications: identification and quantification of long lifetime chemical species and production/consumption mechanisms. *Water Res*. 2018;133:47-59.
- [39] Kondeti S, Phan CQ, Wende K, Jablonowski H, Gangal U, Granick JL, et al. Long-lived and short-lived reactive species produced by a cold atmospheric pressure plasma jet for the inactivation of *Pseudomonas aeruginosa* and *Staphylococcus aureus*. *Free Radic Biol Med*. 2018;124(1):275-87.
- [40] Radi R. Peroxynitrite, a stealthy biological oxidant. *J Biol Chem*. 2013;288(37):26464-72.